

Supporting Information  
for

## Lithium Recognition Reconfigures a Multistep Spin-Crossover Pathway in a Crown Ether-Functionalized Hofmann Framework

Hong-Tai Chen, Yu-Xiao Chen, Meng Yu\* and Jun Tao\*

*Key Laboratory of Cluster Science of Ministry of Education, School of Chemistry and Chemical Engineering, Liangxiang Campus, Beijing Institute of Technology, Beijing 102488, Peoples' Republic of China.*

Email: mengyu@bit.edu.cn; Email: taojun@bit.edu.cn

### Contents

<b>Experimental Details</b> .....	3
<b>Materials and methods</b> .....	3
<b>Adsorption experiments details</b> .....	3
<b>DFT calculation</b> .....	3
<b>Synthesis of crown ether functionalized 11,14-Bis(4-pyridyl)benzo-12-crown-4 (DPy-B12C4)</b> .....	4
<b>Single-crystal X-Ray crystallography</b> .....	5
<b>Synthesis of [Fe(DPy-B12C4)(Ag(CN)<sub>2</sub>)<sub>2</sub>]·2(CH<sub>2</sub>Cl<sub>2</sub>) (1·2CH<sub>2</sub>Cl<sub>2</sub>)</b> .....	6
<b>Additional Tables</b> .....	7
<b>Table S1</b> . Crystallographic data and refinement details for <b>1·2CH<sub>2</sub>Cl<sub>2</sub></b> .....	7
<b>Table S2</b> . Selected bond lengths and angles for compound <b>1·2CH<sub>2</sub>Cl<sub>2</sub></b> at various temperatures .....	7
<b>Table S3</b> . Structural parameters for <b>1·CH<sub>2</sub>Cl<sub>2</sub></b> at various temperatures .....	8
<b>Table S4</b> . The interaction between CH <sub>2</sub> Cl <sub>2</sub> molecules and host framework of <b>1·CH<sub>2</sub>Cl<sub>2</sub></b> at various temperatures .....	8

<b>Table S5.</b> The capture performance of <b>1·CH<sub>2</sub>Cl<sub>2</sub></b> toward different metal ions determined by ICP analysis. ....	8
<b>Table S6.</b> Cartesian coordinates of the optimized structure of <b>1</b> . ....	8
<b>Table S7.</b> Cartesian coordinates of the optimized structure of <b>1+Li<sup>+</sup></b> . ....	10
<b>Table S8.</b> Cartesian coordinates of the optimized structure of <b>1+Mg<sup>2+</sup></b> . ....	11
<b>Table S9.</b> Cartesian coordinates of the optimized structure of <b>1+Na<sup>+</sup></b> . ....	13
<b>Additional Figures</b> .....	15
<b>Fig. S1</b> The FT-IR spectra of <b>1·CH<sub>2</sub>Cl<sub>2</sub></b> . ....	15
<b>Fig. S2</b> Powder X-ray diffraction data of <b>1·CH<sub>2</sub>Cl<sub>2</sub></b> and desolvated <b>1</b> . ....	15
<b>Fig. S3</b> TG curve for <b>1·CH<sub>2</sub>Cl<sub>2</sub></b> and desolvated <b>1</b> . ....	16
<b>Fig. S4</b> (a) The asymmetric unit of <b>1·CH<sub>2</sub>Cl<sub>2</sub></b> (symmetric code: A: -x, y, 1+z; B: -1x, y, z; C: x, 1+y, z); (b) the argentophilic interactions in <b>1·CH<sub>2</sub>Cl<sub>2</sub></b> . ....	16
<b>Fig. S5</b> Powder X-ray diffraction data of <b>1·CH<sub>2</sub>Cl<sub>2</sub></b> before (black) and after (red) Li <sup>+</sup> adsorption. ....	17
<b>Fig. S6</b> Adsorption kinetics curve of <b>1·2CH<sub>2</sub>Cl<sub>2</sub></b> for Li <sup>+</sup> ion (condition: C <sub>0</sub> = 0.5M; T = 300 K; Solvent = DCM/MeOH (1:1)). ....	17
<b>Fig. S7</b> Magnetic susceptibility curves of <b>1·2CH<sub>2</sub>Cl<sub>2</sub></b> after immersion in Na <sup>+</sup> (a) and Mg <sup>2+</sup> (b) solutions. ....	18
<b>Fig. S8</b> The first-order derivative of $\chi^{MT}$ product for <b>1+Li<sup>+</sup></b> . ....	19
<b>Fig. S9</b> PXRD patterns of <b>1</b> upon Li <sup>+</sup> adsorption and desorption. ....	19
<b>Fig. S10.</b> FTIR spectra of free DPy-B12C4 ligand before and after Li <sup>+</sup> adsorption. ....	20
<b>References</b> .....	22

## Experimental Details

### Materials and methods

All reagents and solvents, unless otherwise noted, are commercially available without further purification.

Elemental analyses (C, H, N) were measured by an EUROVECTER EA3000 analyzer. PXRD measurements were recorded using a Bruker D8 Advance Diffractometer with Cu  $K\alpha$  radiation ( $\lambda = 1.54056 \text{ \AA}$ ) between  $5$  and  $50^\circ$  ( $2\theta$ ). The simulated patterns were calculated from the single crystal data. IR spectra were recorded in the range of  $400\text{--}4000 \text{ cm}^{-1}$  on a Thermo IS5 spectrophotometer with KBr pellets. TG measurements were performed on freshly crystals using the TGDTA 6200 instrument in nitrogen atmosphere over a temperature range of  $25\text{--}800 \text{ }^\circ\text{C}$  with a heating rate of  $10 \text{ }^\circ\text{C}/\text{min}$ . DSC analyses were conducted on PerkinElmer DSC 8000 in a closed aluminum pan. The chemical states of elements were obtained by X-ray photoelectron spectroscopy (XPS, Axis Supra), during which Al  $K\alpha$  as chosen as the excitation source.

### Adsorption experiments details.

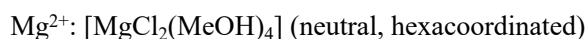
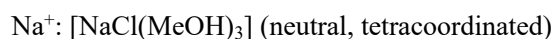
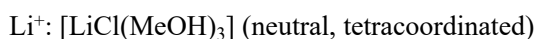
Typical adsorption experiments were conducted by placing the MOF sample (10 mg) into a 10 mL glass vial, followed by the addition of 5 mL of a 0.5 M LiCl solution in methanol/dichloromethane (1:1, v/v). The vial was then agitated on a shaker at room temperature for a predetermined period. After adsorption, the solid sample was collected by centrifugation or filtration and thoroughly washed with fresh methanol/dichloromethane (1:1) to remove residual ions from the surface. The collected solid was subsequently digested with an appropriate amount of concentrated  $\text{HNO}_3$  and diluted to a known volume with deionized water. The concentration of  $\text{Li}^+$  in the resulting solution was determined by inductively coupled plasma optical emission spectrometry (ICP-OES). Adsorption experiments for  $\text{Na}^+$  and  $\text{Mg}^{2+}$  were performed following an analogous procedure, using 0.1 M solutions of NaCl and  $\text{MgCl}_2$ , respectively, in methanol/dichloromethane (1:1). To enhance the solubility of these two salts, a minimal amount of deionized water was added to the solutions.

### DFT calculation

All density functional theory (DFT) calculations were performed using the Gaussian 16

software package at the RB3LYP/6-311+G.<sup>1</sup> To simulate the experimental solvent environment (methanol/dichloromethane, 1:1 v/v mixed solvent), the SMD implicit solvation model was adopted. Since standard implicit solvation models do not support mixed solvents, custom solvent parameters were applied with a dielectric constant of  $\epsilon = 18.5$  to approximate the 1:1 methanol/dichloromethane mixture. All species (including host, guest, and complex) were fully optimized under the same solvation model, and frequency analyses were performed to confirm that all optimized structures correspond to true minima on the potential energy surface (no imaginary frequencies).

To more accurately reflect the speciation of ions in the mixed solvent, a mixed coordination model incorporating both chloride ions and methanol molecules was employed for the metal ions. Based on the coordination preferences of ions in the mixed solvent, the following initial guest structures were constructed:

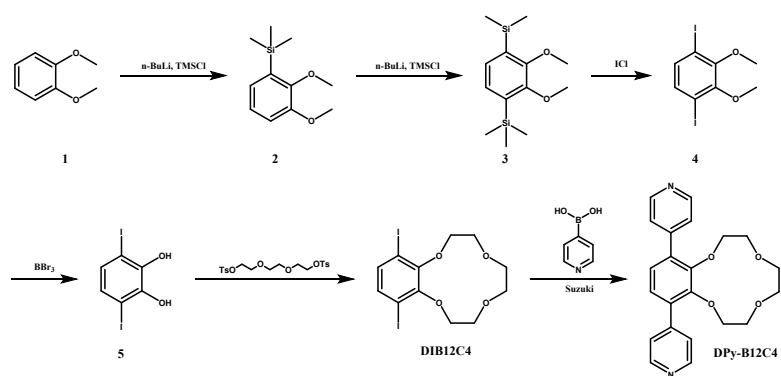


Binding energies  $\Delta E_{bind}$  were calculated according to the following equation:

$$\Delta E_{bind} = E_{complex} + m \times E_{MeOH} + n \times E_{Cl^-} - [E_{host} + E_{guest}] \quad (1)$$

where  $m$  represents the number of methanol molecules released from the first coordination shell of the metal ion during the binding process ( $\text{Li}^+$ :  $m = 3$ ,  $\text{Na}^+$ :  $m = 3$ ,  $\text{Mg}^{2+}$ :  $m = 4$ , and  $n$  denotes the number of chloride ions ( $\text{Li}^+$ :  $n = 1$ ,  $\text{Na}^+$ :  $n = 1$ ,  $\text{Mg}^{2+}$ :  $n = 2$ ). All energy values were obtained as electronic energies (single-point calculations) at the same theoretical level, and basis set superposition error (BSSE) was corrected using the counterpoise method.

#### **Synthesis of crown ether functionalized 11,14-Bis(4-pyridyl)benzo-12-crown-4 (DPy-B12C4).**



**DIB12C4** was synthesized according to the reported procedure.<sup>2</sup> The obtained <sup>1</sup>H NMR spectra matched well with those reported previously. <sup>1</sup>H NMR (500 MHz, CDCl<sub>3</sub>): δ (ppm) = 7.27 (s, 2H), 4.21 (t, J = 4.1, 4H), 3.93 (t, J = 4.1, 4H), 3.82 (s, 4H).

Crown ether functionalized 11,14-Bis(4-pyridyl)benzo-12-crown-4 (**DPy-B12C4**) was obtained through the Suzuki coupling reaction between **DIB12C4** and pyridin-4-ylboronic acid. The experimental procedures are as follows:

**DIB12C4** (0.5 mmol, 238 mg), K<sub>2</sub>CO<sub>3</sub> (345 mg, 5.0 equiv.), pyridin-4-ylboronic acid (154 mg, 2.5 equiv.), and Pd(PPh<sub>3</sub>)<sub>4</sub> (60 mg, 0.1 equiv.) were added into a two-necked flask. A degassed mixture of 1,4-dioxane (12 mL) and H<sub>2</sub>O (3 mL) was added into the flask under N<sub>2</sub> atmosphere. The reaction mixture was heated to reflux at 100 °C for 24 h. After cooling to room temperature, the solvent was evaporated under reduced pressure and the residue was diluted with H<sub>2</sub>O (20 mL), extracted with CH<sub>2</sub>Cl<sub>2</sub> (3 × 50 mL). The combined organic layer was washed with brine, dried over Na<sub>2</sub>SO<sub>4</sub>, and then evaporated to dryness. The crude product was purified by flash column chromatography on silica gel with DCM/MeOH (20:1) as the eluent to give the product **DPy-B12C4**. Yield: 158 mg (83.5%). <sup>1</sup>H NMR (500 MHz, CDCl<sub>3</sub>): δ (ppm) = 8.61 (s, 4H), 7.50 (s, 4H), 7.17 (s, 2H), 3.87 (s, 4H), 3.72 (s, 4H), 3.68 (s, 4H). <sup>13</sup>C NMR (500 MHz, CDCl<sub>3</sub>): δ (ppm) = 150.78, 149.82, 145.52, 134.42, 125.79, 123.89, 77.31, 77.06, 76.80, 74.95, 73.56, 70.75, 70.15. HRMS (EI): Calculated for C<sub>22</sub>H<sub>22</sub>O<sub>4</sub>N<sub>2</sub> [M]<sup>+</sup>: 379.16; Found: 379.15. Mp: 225.5 °C

### Single-crystal X-Ray crystallography.

Single-crystal X-ray diffraction experiments of **1·2CH<sub>2</sub>Cl<sub>2</sub>** (100 K, 180K, and 273 K) were performed on a Rigaku Oxford XtaLAB PRO diffractometer (Mo Kα, λ = 0.71073 Å) equipped with an Oxford Cryosystems Cryostream 800 apparatus. Structure solution and refinement were carried out by using the SHELXL program package and the non-hydrogen atoms (Fe, O, N, C)

were refined anisotropically by full-matrix least-squares techniques based on  $F^2$  values.<sup>3,4</sup> Hydrogen atoms were fixed geometrically at calculated positions and allowed to ride on the parent atoms. The relevant crystallographic data and structural refinement details for **1·2CH<sub>2</sub>Cl<sub>2</sub>** (100 K, 180K, and 273 K) were summarized in [Table S1](#). Selected bond lengths and angles for **1·2CH<sub>2</sub>Cl<sub>2</sub>** (100 K, 180K, and 273 K) were listed in [Table S2](#). Structural parameters for **1·2CH<sub>2</sub>Cl<sub>2</sub>** (100 K, 180K, and 273 K) were listed in [Table S3](#). The dihedral angle between pyridine and fused rings of **1·2CH<sub>2</sub>Cl<sub>2</sub>** (100 K, 180K, and 273 K) at various temperatures were listed in [Table S4](#). Full crystallographic data have been deposited under deposition numbers CCDC 2536196–2536198.

#### **Synthesis of [Fe(DPy-B12C4)(Ag(CN)<sub>2</sub>)<sub>2</sub>]·2(CH<sub>2</sub>Cl<sub>2</sub>) (1·2CH<sub>2</sub>Cl<sub>2</sub>).**

**1·2CH<sub>2</sub>Cl<sub>2</sub>** was synthesized using a liquid-liquid diffusion method in a test tube (8 mm inner diameter). A mixed solution of methanol/CH<sub>2</sub>Cl<sub>2</sub> (2 mL, v/v = 1:1) containing DPy-B12C4 (0.025 mmol, 9.5 mg) and NaAg(CN)<sub>2</sub> (0.05 mmol, 9.2 mg) was placed at the bottom, upon which a mixture of methanol and CH<sub>2</sub>Cl<sub>2</sub> (2 mL, v/v = 1:2) was added as buffer and then a methanol solution (2 mL) of Fe(ClO<sub>4</sub>)<sub>2</sub>·6H<sub>2</sub>O (0.025 mmol, 9.1 mg) was layered on the top. The test tube was sealed and put aside for one week; light yellow crystals were obtained. For DPy-B12C4, yield: ~52% (based on DPy-B12C4 ligand). FT-IR (KBr pellet, cm<sup>-1</sup>): 432, 727, 809, 899, 939, 1034, 1118, 1209, 1353, 1407, 1608, 2163, 2360, 2851, 3399.

## Additional Tables

**Table S1.** Crystallographic data and refinement details for **1·2CH<sub>2</sub>Cl<sub>2</sub>**.

T / K	273	180	100
Empirical formula	C <sub>28</sub> H <sub>25</sub> Ag <sub>2</sub> Cl <sub>4</sub> FeN <sub>6</sub> O <sub>4</sub>	C <sub>28</sub> H <sub>25</sub> Ag <sub>2</sub> Cl <sub>4</sub> FeN <sub>6</sub> O <sub>4</sub>	C <sub>28</sub> H <sub>25</sub> Ag <sub>2</sub> Cl <sub>4</sub> FeN <sub>6</sub> O <sub>4</sub>
Molecular weight	923.23	923.23	923.23
Crystal system	triclinic	triclinic	triclinic
Space group	<i>P</i> $\bar{1}$	<i>P</i> $\bar{1}$	<i>P</i> $\bar{1}$
<i>a</i> /Å	10.6155(2)	10.6003(3)	10.4318(3)
<i>b</i> /Å	10.7142(3)	10.7047(4)	10.5213(3)
<i>c</i> /Å	15.8128(3)	15.7978(5)	15.6031(4)
$\alpha$ /°	86.857(2)	86.570(3)	87.313(2)
$\beta$ /°	82.786(2)	82.215(2)	83.349(2)
$\gamma$ /°	80.949(2)	80.095(2)	81.286(2)
<i>V</i> /Å <sup>3</sup>	1760.91(7)	1748.40(10)	1680.63(8)
<i>Z</i>	2	2	2
$\rho_{\text{calc}}/\text{cm}^3$	1.741	1.753	1.824
$\mu/\text{mm}^{-1}$	1.852	1.865	1.941
<i>F</i> (000)	911.0	910.0	910.0
Goodness-of-fit on <i>F</i> <sup>2</sup>	1.044	1.042	1.051
<i>R</i> <sub>1</sub> [ <i>I</i> ≥ 2σ( <i>I</i> )] <sup>a</sup>	0.0387	0.0390	0.0489
<i>wR</i> <sub>2</sub> (all data) <sup>b</sup>	0.1088	0.1048	0.1363
<i>R</i> <sub>int</sub> /%	0.0327	0.0380	0.0365
CCDC No.	2536198	2536197	2536196

$${}^a R_1 = \sum |F_o| - |F_c| / \sum |F_o|; {}^b wR_2 = [\sum w(F_o^2 - F_c^2)^2] / \sum w(F_o^2)^2]^{1/2}$$

**Table S2.** Selected bond lengths and angles for compound **1·2CH<sub>2</sub>Cl<sub>2</sub>** at various temperatures.

	273 K	180 K	100
Fe1–N2#2	2.230(2)	2.224(2)	2.113(4)
Fe1–N1	2.228(2)	2.222(2)	2.099(4)
Fe1–N6#3	2.136(2)	2.129(2)	2.013(4)
Fe1–N4	2.132(2)	2.128(2)	2.025(4)
Fe1–N3	2.169(3)	2.175(3)	2.058(4)
Fe1–N54	2.177(3)	2.164(3)	2.049(4)
N1–Fe1–N2#2	174.39(9)	174.48(9)	174.15(14)
N6#3–Fe1–N2#2	92.41(9)	92.40(9)	92.59(14)
N6#3–Fe1–N1	89.25(9)	89.24(9)	88.99(14)
N6#3–Fe1–N3	89.61(11)	87.68(10)	88.45(15)
N6#3–Fe1–N5#4	87.64(11)	89.78(10)	89.52(14)
N4–Fe1–N2#2	91.42(9)	91.57(9)	91.03(14)
N4–Fe1–N1	87.35(9)	87.21(9)	87.74(14)
N4–Fe1–N6#3	174.17(10)	174.09(10)	175.56(13)
N4–Fe1–N3	94.86(11)	87.85(11)	95.14(15)
N4–Fe1–N5#4	87.87(11)	94.68(11)	86.91(16)
N3–Fe1–N2#2	89.00(9)	91.34(9)	90.61(14)
N3–Fe1–N1	85.66(9)	93.99(9)	93.58(14)
N3–Fe1–N5#4	177.22(10)	177.46(10)	177.95(15)
N5#4–Fe1–N2#2	91.49(9)	86.04(9)	89.20(14)
N5#4–Fe1–N1	93.92(10)	88.70(9)	86.66(14)

Symmetric code: #1: 1-x, 1-y, 2-z; #2: +x, +y, 1+z; #3: -1+x, +y, +z; #4: +x, 1+y, +z.

**Table S3.** Structural parameters for **1·CH<sub>2</sub>Cl<sub>2</sub>** at various temperatures.

	273K	180K	100K
Fe–N <sub>av</sub> (Å) <sup>a</sup>	2.179	2.174	2.059
Σ (°) <sup>b</sup>	27.702	27.460	25.469
Θ (°) <sup>c</sup>	94.873	93.248	89.696
Vol (Å <sup>3</sup> ) <sup>d</sup>	13.730	13.650	11.600

<sup>a</sup>Fe–N<sub>av</sub>: the average Fe–N bond lengths; <sup>b</sup>Σ<sub>Fe</sub> (octahedral distortion parameters): the sum of the deviations of N–Fe–N angles from 90°; <sup>c</sup>Θ: The sum of the deviation of 24 unique torsional angles between the ligand atoms on opposite triangular faces of the octahedron viewed along the pseudo-threefold axis from 60°; <sup>d</sup>Vol: the volume of the [FeN<sub>6</sub>] octahedron.

**Table S4.** The interaction between CH<sub>2</sub>Cl<sub>2</sub> molecules and host framework of **1**·CH<sub>2</sub>Cl<sub>2</sub> at various temperatures.

<b>1</b> ·CH <sub>2</sub> Cl <sub>2</sub>	273K	180K	100K
d <sub>π</sub> 1 (Å) <sup>a</sup>	3.746	3.738	3.527
d <sub>π</sub> 2 (Å)	3.857	3.817	3.642
d <sub>π</sub> 3 (Å)	3.985	3.941	3.785
d <sub>Ag</sub> 1 (Å) <sup>b</sup>	3.387	3.356	3.242
d <sub>Ag</sub> 2 (Å)	3.412	3.384	3.223

<sup>a</sup>d<sub>π</sub>: the distance of Cl··π interactions; <sup>b</sup>d<sub>Ag</sub>: the distance of Cl··Ag(I) interactions.

**Table S5.** The capture performance of **1**·CH<sub>2</sub>Cl<sub>2</sub> toward different metal ions determined by ICP analysis.

	Li <sup>+</sup> / mg g <sup>-1</sup>	Na <sup>+</sup> / mg g <sup>-1</sup>	Mg <sup>2+</sup> / mg g <sup>-1</sup>
C <sub>0</sub> = 0.5M	12.4		
C <sub>0</sub> = 0.1M	9.7	1.1	0.7

Condition: C<sub>0</sub> = the initial concentration, room temperature, 24h, Solvent = DCM/MeOH (1:1).

**Table S6.** Cartesian coordinates of the optimized structure of **1**.

Atom number	Element	X	Y	Z
1	N	-8.5293	0.710253	-1.70942
2	C	-8.60636	1.528574	-2.56852
3	Fe	-8.27989	-0.71318	-0.05229
4	N	-10.2807	-0.79043	0.032814
5	N	-8.2259	-2.0961	1.581893
6	N	-8.39492	0.965424	1.334516
7	C	-8.2213	-2.88033	2.475122
8	C	-8.48961	1.90001	2.006119
9	C	-10.9187	-0.84883	1.228579
10	H	-10.286	-0.90469	2.096313
11	C	-11.0233	-0.79003	-1.10218
12	H	-10.4753	-0.67901	-2.02065
13	C	-13.0711	-0.9103	0.155344
14	C	-12.3057	-0.90744	1.3224
15	H	-12.7688	-0.96662	2.296364
16	C	-12.4131	-0.85102	-1.07399
17	H	-12.9629	-0.83457	-2.00355
18	N	-8.35594	-2.34786	-1.46099
19	C	-8.39382	-3.24345	-2.18899
20	N	8.007661	0.453083	-1.53516
21	C	8.059807	1.187894	-2.42478
22	Fe	8.086283	-0.91351	0.076342
23	O	-1.37188	1.781766	-0.06582

24	O	1.370696	1.67766	-0.13467
25	N	-6.00135	-0.67958	-0.09919
26	N	5.821942	-0.92568	0.119679
27	N	8.365831	-2.35285	1.75067
28	N	8.201993	0.709823	1.507297
29	O	-0.67761	4.673741	0.013457
30	C	8.516588	-3.01735	2.682745
31	C	-3.09137	-0.63847	-0.0691
32	C	0.662603	0.478365	-0.07917
33	C	-5.26298	-1.66987	0.48058
34	H	-5.83368	-2.44372	0.969674
35	C	-5.27947	0.325029	-0.6733
36	H	-5.86235	1.086853	-1.16905
37	C	-0.75995	0.518646	-0.05651
38	C	-1.56578	-0.64763	-0.04593
39	C	-3.86043	-1.67788	0.509438
40	H	-3.3819	-2.49674	1.027777
41	C	-3.8766	0.375584	-0.6757
42	H	-3.39711	1.209507	-1.15876
43	O	2.388008	4.399114	-0.15554
44	C	8.299609	1.557624	2.335191
45	C	5.12966	0.158663	0.57486
46	H	5.733965	0.949654	0.991727
47	C	1.394801	-0.73274	0.012853
48	C	5.05632	-1.94712	-0.36231
49	H	5.605093	-2.78926	-0.75579
50	C	-0.82065	-1.85301	0.01105
51	H	-1.34833	-2.79667	0.010948
52	C	2.91721	-0.7922	0.0524
53	C	3.730205	0.256217	0.552657
54	H	3.277884	1.160178	0.925135
55	C	0.579948	-1.89138	0.059884
56	H	1.051716	-2.86076	0.142282
57	C	3.653648	-1.91326	-0.40573
58	H	3.15179	-2.76658	-0.83973
59	C	-1.25789	2.583294	1.174319
60	H	-0.23095	2.546344	1.534937
61	H	-1.93196	2.152524	1.919083
62	C	-1.67319	3.997914	0.831165
63	H	-2.59049	3.984569	0.245622
64	H	-1.85646	4.559361	1.754173
65	C	0.334211	5.428622	0.745188
66	H	0.625244	4.910829	1.662825
67	C	1.55901	5.595449	-0.12961
68	H	1.261787	5.892148	-1.14002
69	H	2.192018	6.376056	0.296079
70	C	1.19743	2.54644	-1.32731
71	H	0.232836	3.037616	-1.27526
72	H	1.259878	1.917285	-2.21921
73	C	2.336194	3.544172	-1.32758
74	H	3.293262	3.026502	-1.33564
75	H	2.257278	4.15496	-2.23655
76	N	8.170755	-2.6042	-1.28723
77	C	8.21201	-3.51083	-2.05521
78	N	10.08712	-0.83868	-0.02834
79	C	12.87595	-0.71541	-0.18235
80	C	10.82356	-1.97138	-0.15092
81	H	10.26469	-2.88552	-0.2411
82	C	10.73054	0.354943	0.018239
83	H	10.10761	1.217419	0.175026
84	C	12.21277	-1.94254	-0.22761
85	H	12.75612	-2.86955	-0.3373
86	C	12.11657	0.449078	-0.05814

87	H	12.58536	1.420622	-0.00391
88	H	13.95453	-0.66776	-0.24175
89	H	-14.1502	-0.95692	0.202634
90	H	-8.63276	2.705732	2.683576
91	H	-8.49704	-4.05101	-2.87156
92	H	8.191099	1.944401	-3.1588
93	H	8.72583	-3.68618	3.481357
94	H	-0.07667	6.411863	1.003207

**Table S7.** Cartesian coordinates of the optimized structure of **1**+Li<sup>+</sup>.

Atom number	Element	X	Y	Z
1	N	8.420459	1.35997	0.502052
2	C	8.503179	2.515551	0.700654
3	Fe	8.166821	-0.7677	0.03611
4	N	10.17317	-0.91596	0.03636
5	N	8.082627	-2.86441	-0.41496
6	N	8.286559	-0.2819	-2.07381
7	C	8.081827	-4.02791	-0.58224
8	C	8.465914	0.050812	-3.16534
9	C	10.8149	-1.63807	-0.91948
10	H	10.19197	-2.12799	-1.64632
11	C	10.92338	-0.3081	0.992398
12	H	10.38785	0.274182	1.720608
13	C	12.96631	-1.14526	0.037026
14	C	12.19839	-1.77203	-0.94585
15	H	12.66026	-2.36487	-1.72106
16	C	12.31024	-0.4015	1.01935
17	H	12.86211	0.106625	1.795879
18	N	8.212219	-1.22043	2.157965
19	C	8.314416	-1.58087	3.250512
20	N	-8.11849	1.206911	0.416102
21	C	-8.19847	2.299067	0.784654
22	Fe	-8.22146	-0.86462	-0.04078
23	O	1.160597	1.85318	-0.06674
24	O	-1.41807	1.740573	0.034097
25	N	5.874694	-0.69168	0.019753
26	N	-5.91899	-0.90781	-0.05588
27	N	-8.51108	-3.01328	-0.49715
28	N	-8.31232	-0.43222	-2.15991
29	C	-8.70753	-4.1012	-0.83066
30	C	2.981519	-0.65014	-0.03016
31	C	-0.75905	0.482696	-0.00523
32	C	5.154259	-1.3185	-0.95197
33	H	5.728752	-1.84367	-1.69811
34	C	5.141219	-0.05656	0.977012
35	H	5.705944	0.43417	1.753986
36	C	0.661451	0.531257	-0.0597
37	C	1.452853	-0.63576	-0.06149
38	C	3.751027	-1.31916	-1.00568
39	H	3.270909	-1.83858	-1.82312
40	C	3.737928	-0.01738	0.983003
41	H	3.244222	0.502878	1.792253
42	O	-1.16181	4.377641	0.227006
43	C	-8.41998	-0.30058	-3.32311
44	C	-5.22665	0.013067	-0.785
45	H	-5.82412	0.672294	-1.39448
46	C	-1.49879	-0.71535	-0.02577
47	C	-5.15532	-1.76794	0.674169
48	H	-5.69491	-2.49461	1.260903
49	C	0.706418	-1.83996	-0.0739
50	H	1.246212	-2.77671	-0.08023
51	C	-3.02367	-0.76815	-0.02956
52	C	-3.82832	0.110884	-0.79214

53	H	-3.37534	0.870929	-1.40861
54	C	-0.69671	-1.88202	-0.06364
55	H	-1.17827	-2.84868	-0.09957
56	C	-3.75111	-1.72847	0.70864
57	H	-3.24134	-2.44392	1.33854
58	C	2.353939	2.278779	-0.84041
59	H	2.20372	2.017231	-1.88918
60	H	3.254824	1.802335	-0.46572
61	C	2.417995	3.77431	-0.62918
62	H	2.572606	4.000484	0.427496
63	H	3.230449	4.205118	-1.21592
64	C	0.698299	5.623124	-0.54969
65	H	0.151862	6.085985	-1.36659
66	C	-0.20525	5.408288	0.658936
67	H	0.348051	5.051876	1.53091
68	H	-0.73286	6.328364	0.912724
69	C	-1.62481	2.317621	1.402892
70	H	-0.67502	2.262503	1.934139
71	H	-2.38055	1.730345	1.922333
72	C	-2.07536	3.75036	1.187887
73	H	-3.06512	3.791716	0.739605
74	H	-2.08989	4.292993	2.134316
75	N	-8.31645	-1.37261	2.07197
76	C	-8.411	-1.59962	3.221423
77	N	-10.2286	-0.72137	-0.01535
78	C	-13.0236	-0.51615	0.008637
79	C	-10.9884	-1.61704	0.667757
80	H	-10.4565	-2.38137	1.20526
81	C	-10.8615	0.276622	-0.68651
82	H	-10.2339	0.951919	-1.24044
83	C	-12.3765	-1.54144	0.700118
84	H	-12.935	-2.27349	1.263959
85	C	-12.2457	0.404766	-0.69557
86	H	-12.7018	1.209074	-1.2532
87	H	-14.1013	-0.43788	0.01686
88	H	14.0432	-1.23431	0.037792
89	H	8.653082	0.372632	-4.16343
90	H	8.4215	-1.93679	4.24894
91	H	-8.30008	3.295667	1.144968
92	H	-8.8993	-5.0984	-1.15283
93	H	1.564341	6.237847	-0.30543
94	Li	-0.32138	3.085269	-0.85091
95	O	1.128646	4.309049	-1.07309

**Table S8.** Cartesian coordinates of the optimized structure of **1+Mg<sup>2+</sup>**.

Atom number	Element	X	Y	Z
1	N	8.446624	1.247815	0.501269
2	C	8.723524	2.356846	0.667319
3	Fe	8.187978	-0.87809	0.037866
4	N	10.20562	-1.02743	0.040566
5	N	8.115112	-2.97874	-0.40799
6	N	8.31492	-0.39897	-2.07157
7	C	8.157108	-4.12432	-0.54852
8	C	8.495546	-0.08202	-3.16752
9	C	10.85869	-1.70964	-0.94321
10	H	10.25161	-2.15227	-1.71358
11	C	10.95852	-0.46226	1.026946
12	H	10.42934	0.070467	1.797639
13	C	13.00534	-1.2594	0.045291
14	C	12.24172	-1.84178	-0.96891
15	H	12.70993	-2.39304	-1.77037
16	C	12.34441	-0.55917	1.057126
17	H	12.89417	-0.0942	1.861508
18	N	8.242504	-1.32987	2.161919

19	C	8.34977	-1.67885	3.257758
20	N	-8.09208	1.069443	0.417585
21	C	-8.19103	2.169012	0.756714
22	Fe	-8.18947	-1.00237	-0.03573
23	O	1.128017	1.909809	-0.0334
24	O	-1.43885	1.741349	0.122496
25	N	5.891314	-0.75616	0.013785
26	N	-5.88488	-1.00974	-0.04854
27	N	-8.47836	-3.153	-0.48791
28	N	-8.28372	-0.57469	-2.1554
29	C	-8.67458	-4.24521	-0.80826
30	C	2.997807	-0.62092	-0.05166
31	C	-0.75468	0.499933	0.041143
32	C	5.1553	-1.31925	-0.9888
33	H	5.709451	-1.81737	-1.7684
34	C	5.16633	-0.13802	0.992996
35	H	5.730509	0.294952	1.804144
36	C	0.665294	0.575127	-0.03874
37	C	1.469595	-0.58835	-0.07951
38	C	3.754326	-1.27385	-1.04888
39	H	3.264902	-1.7439	-1.89003
40	C	3.766162	-0.05493	0.991364
41	H	3.2836	0.439025	1.822874
42	O	-1.25925	4.411612	0.35691
43	C	-8.43017	-0.48314	-3.29744
44	C	-5.20914	-0.03997	-0.73388
45	H	-5.81166	0.648937	-1.30396
46	C	-1.47097	-0.71323	-0.00691
47	C	-5.09858	-1.88416	0.644456
48	H	-5.61019	-2.66302	1.187764
49	C	0.741468	-1.80265	-0.11874
50	H	1.291366	-2.73274	-0.15697
51	C	-2.99236	-0.7995	-0.00806
52	C	-3.81591	0.091937	-0.73344
53	H	-3.38081	0.892303	-1.30988
54	C	-0.65752	-1.86731	-0.09281
55	H	-1.12256	-2.84082	-0.15493
56	C	-3.69711	-1.81014	0.684126
57	H	-3.17081	-2.54438	1.27713
58	C	2.270913	2.411571	-0.84433
59	H	2.091706	2.167721	-1.8927
60	H	3.20207	1.96196	-0.51389
61	C	2.296378	3.90861	-0.6067
62	H	2.478284	4.120861	0.448837
63	H	3.07916	4.370828	-1.2101
64	C	0.543034	5.725953	-0.45093
65	H	-0.03383	6.1887	-1.24639
66	C	-0.31836	5.465946	0.77908
67	H	0.270491	5.108957	1.627282
68	H	-0.86262	6.365472	1.066745
69	C	-1.61321	2.309747	1.506908
70	H	-0.64377	2.275528	2.002385
71	H	-2.33048	1.694463	2.048055
72	C	-2.11426	3.73509	1.334657
73	H	-3.12205	3.757473	0.926691
74	H	-2.10882	4.256405	2.292921
75	N	-8.28592	-1.50734	2.078187
76	C	-8.41952	-1.72186	3.20522
77	N	-10.2089	-0.86366	-0.01432
78	C	-13.0112	-0.66345	0.002488
79	C	-10.9784	-1.79004	0.624665
80	H	-10.4616	-2.59656	1.114077
81	C	-10.8468	0.163336	-0.64526
82	H	-10.2269	0.884321	-1.14948
83	C	-12.3661	-1.71868	0.650949
84	H	-12.929	-2.47944	1.170382
85	C	-12.2304	0.290063	-0.65515
86	H	-12.6865	1.121343	-1.17132

87	H	-14.0885	-0.58729	0.007932
88	H	14.08167	-1.34922	0.047558
89	H	8.678579	0.204673	-4.18229
90	H	8.46397	-2.0007	4.272171
91	H	-8.30405	3.185924	1.067698
92	H	-8.87056	-5.25604	-1.10047
93	H	1.399503	6.358138	-0.21953
94	Mg	-0.43006	3.178165	-0.78646
95	O	0.989042	4.425524	-1.00728

**Table S9.** Cartesian coordinates of the optimized structure of **1+Na<sup>+</sup>**.

Atom number	Element	X	Y	Z
1	N	8.412754	0.929173	1.308919
2	C	8.318557	1.947697	1.903214
3	Fe	8.178353	-0.86966	0.059964
4	N	10.17751	-0.986	0.0077
5	N	8.076906	-2.61163	-1.17103
6	N	8.279767	0.411607	-1.70158
7	C	7.88941	-3.55937	-1.85273
8	C	8.482559	1.141226	-2.57332
9	C	10.81385	-1.57471	-1.04227
10	H	10.17565	-2.0044	-1.79449
11	C	10.92868	-0.48766	1.028018
12	H	10.38063	0.019556	1.802661
13	C	12.97018	-1.16798	-0.05243
14	C	12.20106	-1.66933	-1.10335
15	H	12.66247	-2.14216	-1.95755
16	C	12.31788	-0.57384	1.028865
17	H	12.87297	-0.16901	1.862057
18	N	8.205585	-2.09099	1.837566
19	C	8.307589	-2.82534	2.722535
20	N	-8.12611	0.81471	1.166568
21	C	-8.17054	1.726582	1.873707
22	Fe	-8.25156	-0.9225	-0.0538
23	O	1.169154	1.791989	-0.06551
24	O	-1.49192	1.644593	-0.03713
25	N	5.871431	-0.81822	0.085807
26	N	-5.92298	-0.97588	-0.08453
27	N	-8.51672	-2.72371	-1.3083
28	N	-8.31903	0.299707	-1.84302
29	C	-8.73741	-3.6005	-2.02596
30	C	2.98011	-0.7609	0.031991
31	C	-0.76536	0.418878	-0.02939
32	C	5.15469	-1.38304	-0.92773
33	H	5.737884	-1.88984	-1.68084
34	C	5.139113	-0.26301	1.095321
35	H	5.711453	0.197646	1.886668
36	C	0.661025	0.468568	-0.06092
37	C	1.447488	-0.71081	-0.02559
38	C	3.749519	-1.36228	-0.98606
39	H	3.268318	-1.81907	-1.83968
40	C	3.734425	-0.23222	1.106168
41	H	3.237467	0.210936	1.958043
42	O	-1.22469	4.578707	0.274119
43	C	-8.18226	0.978813	-2.80106
44	C	-5.22873	-0.06623	-0.82909
45	H	-5.83215	0.566142	-1.46363
46	C	-1.50081	-0.78688	-0.03534
47	C	-5.16815	-1.83018	0.664057
48	H	-5.72357	-2.51965	1.282463
49	C	0.696764	-1.91176	-0.04065
50	H	1.236561	-2.84883	-0.02949
51	C	-3.0303	-0.84322	-0.05105

52	C	-3.82935	0.026186	-0.82988
53	H	-3.37186	0.777296	-1.45346
54	C	-0.70265	-1.95441	-0.05087
55	H	-1.18733	-2.92024	-0.07996
56	C	-3.76147	-1.79392	0.697678
57	H	-3.25355	-2.50285	1.336715
58	C	2.396427	2.27996	-0.73709
59	H	2.312704	2.111956	-1.81235
60	H	3.27266	1.765354	-0.35908
61	C	2.517651	3.747592	-0.3849
62	H	2.538048	3.86624	0.699595
63	H	3.450496	4.126495	-0.80492
64	C	0.899002	5.678359	-0.24058
65	H	0.439844	6.29085	-1.01212
66	C	-0.10568	5.339243	0.864602
67	H	0.368655	4.775052	1.673271
68	H	-0.48864	6.276724	1.271691
69	C	-1.66554	2.300218	1.288146
70	H	-0.72044	2.229639	1.829522
71	H	-2.43481	1.765817	1.846836
72	C	-2.10449	3.757624	1.133062
73	H	-3.08678	3.842984	0.677414
74	H	-2.14461	4.174729	2.143023
75	N	-8.323	-2.20462	1.69552
76	C	-8.15743	-2.86793	2.660311
77	N	-10.2564	-0.79763	0.030147
78	C	-13.0509	-0.63012	0.139959
79	C	-10.9921	-1.78722	0.608507
80	H	-10.4277	-2.58668	1.054732
81	C	-10.912	0.275274	-0.49369
82	H	-10.2952	1.002154	-0.99163
83	C	-12.3817	-1.73469	0.667736
84	H	-12.9217	-2.54642	1.132065
85	C	-12.2981	0.389324	-0.44417
86	H	-12.7728	1.260251	-0.87126
87	H	-14.1292	-0.56604	0.181466
88	H	14.04853	-1.23916	-0.07523
89	H	8.65359	1.772958	-3.41392
90	H	8.427241	-3.4495	3.57773
91	H	-8.20363	2.628561	2.438688
92	H	-8.97924	-4.41833	-2.66444
93	H	1.724318	6.238702	0.204372
94	Na	-0.32236	3.16825	-1.08283
95	O	1.399767	4.503961	-0.96458

## Additional Figures

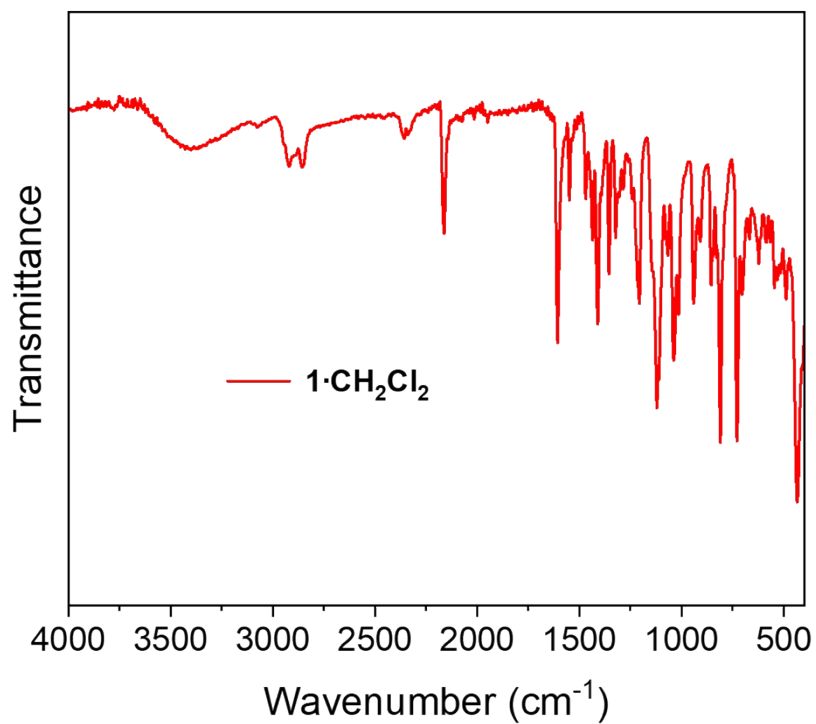


Fig. S1 The FT-IR spectra of 1·CH<sub>2</sub>Cl<sub>2</sub>.

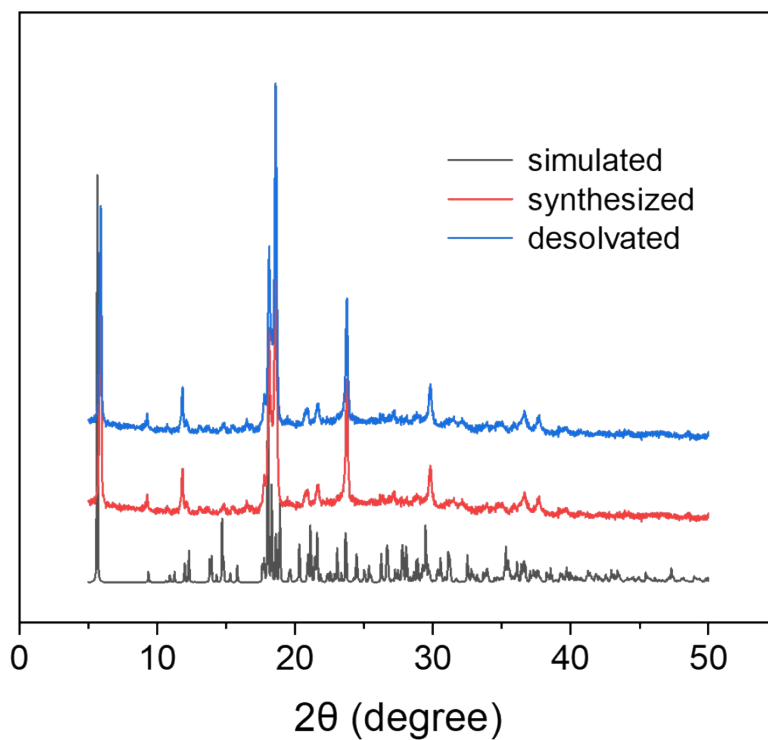


Fig. S2 Powder X-ray diffraction data of 1·CH<sub>2</sub>Cl<sub>2</sub> and desolvated 1.

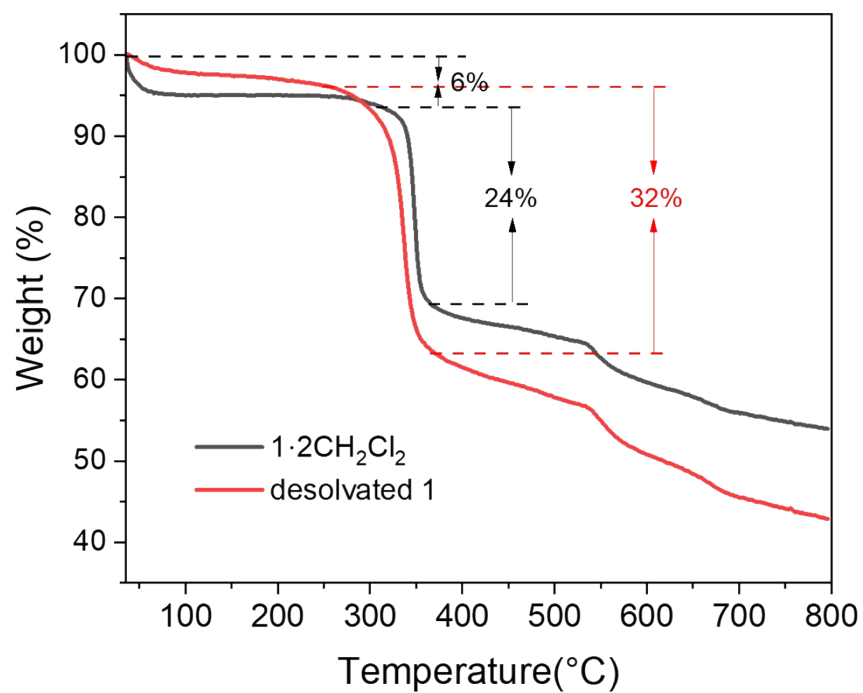


Fig. S3 TG curve for  $1 \cdot \text{CH}_2\text{Cl}_2$  and desolvated **1**.

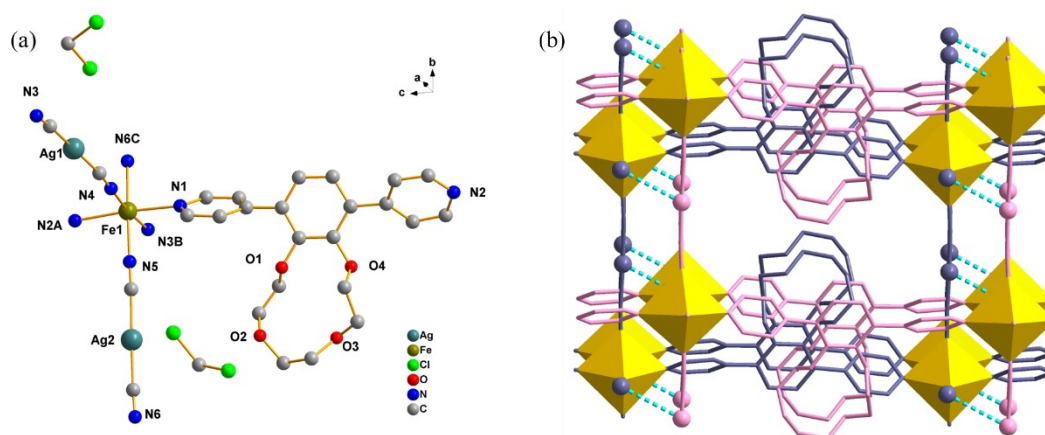
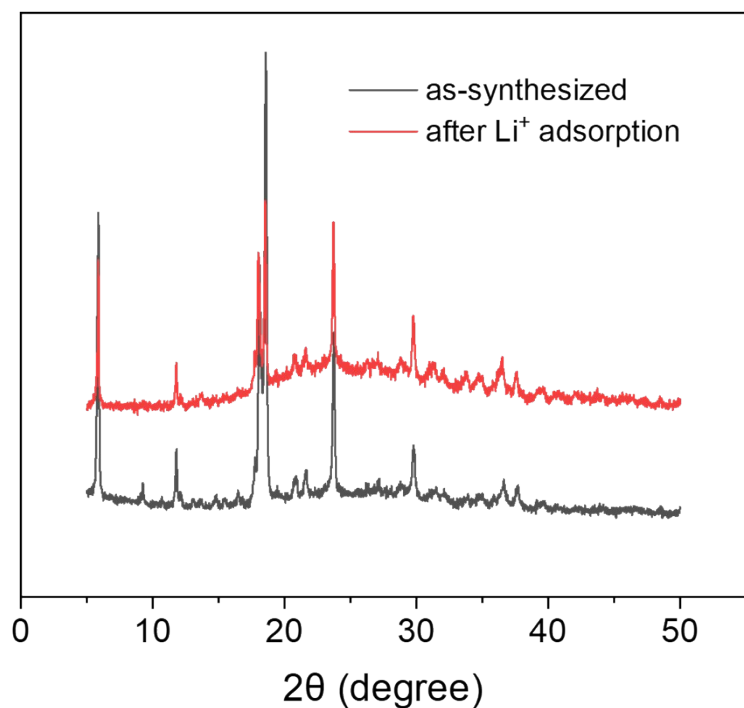
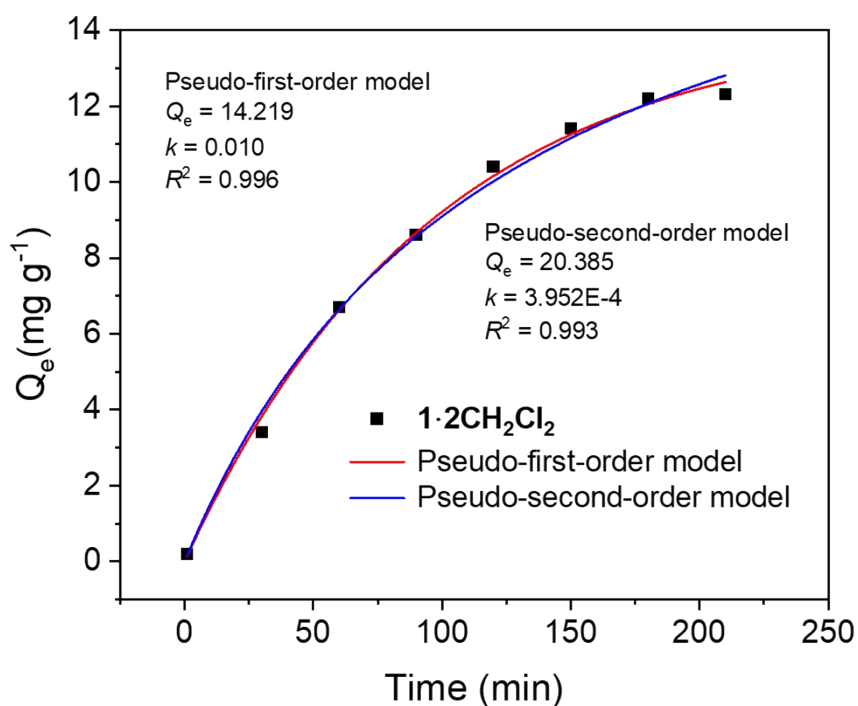


Fig. S4 (a) The asymmetric unit of  $1 \cdot \text{CH}_2\text{Cl}_2$  (symmetric code: A:  $-x, y, 1+z$ ; B:  $-1x, y, z$ ; C:  $x, 1+y, z$ ); (b) the argentophilic interactions in  $1 \cdot \text{CH}_2\text{Cl}_2$ .



**Fig. S5** Powder X-ray diffraction data of  $1 \cdot \text{CH}_2\text{Cl}_2$  before (black) and after (red)  $\text{Li}^+$  adsorption.



**Fig. S6** Adsorption kinetics curve of  $1 \cdot 2\text{CH}_2\text{Cl}_2$  for  $\text{Li}^+$  ion (condition:  $C_0 = 0.5\text{M}$ ;  $T = 300\text{ K}$ ; Solvent = DCM/MeOH (1:1)).

To elucidate the kinetic mechanism of the  $\text{Li}^+$  ions adsorption process, the adsorption data were fitted using pseudo-first-order and pseudo-second-order kinetic models. The two kinetic models

are described as the following equations:

$$Q_t = Q_e(1 - e^{-k_1 t}) \quad (2)$$

$$Q_t = \frac{k_2 Q_e^2 t}{1 + k_2 Q_e t} \quad (3)$$

where  $Q_t$  and  $Q_e$  refer to  $\text{Li}^+$  ion adsorption amount at  $t$  (min) and equilibrium time;  $k_1$  and  $k_2$  are the rate constants of the pseudo-first-order kinetic model and the pseudo-second-order kinetic model. The fitting results indicate that both models provide satisfactory descriptions of the entire adsorption process, with high correlation coefficients ( $R^2 > 0.99$ ). The good fit of the pseudo-first-order model suggests a potential contribution from physical diffusion processes during the initial stage of adsorption, while the excellent agreement with the pseudo-second-order model reveals that chemisorption is the predominant rate-controlling mechanism throughout the process. This finding is consistent with the specific binding of  $\text{Li}^+$  ions through ion-dipole interactions with the crown ether moieties, which is characteristic of chemisorption. The applicability of both models in describing the adsorption behavior reflects a synergistic effect involving both physical diffusion and chemical complexation during the adsorption process.

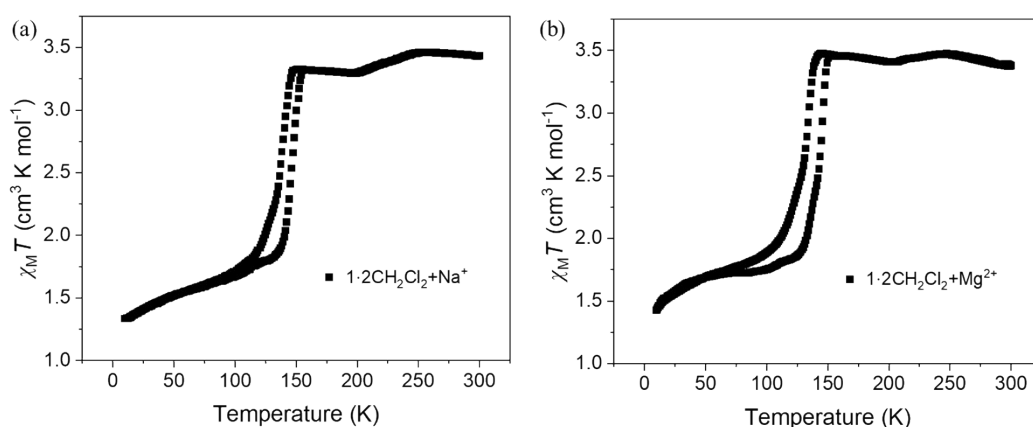


**Fig. S7** Magnetic susceptibility curves of  $1:2\text{CH}_2\text{Cl}_2$  after immersion in  $\text{Na}^+$  (a) and  $\text{Mg}^{2+}$  (b) solutions.

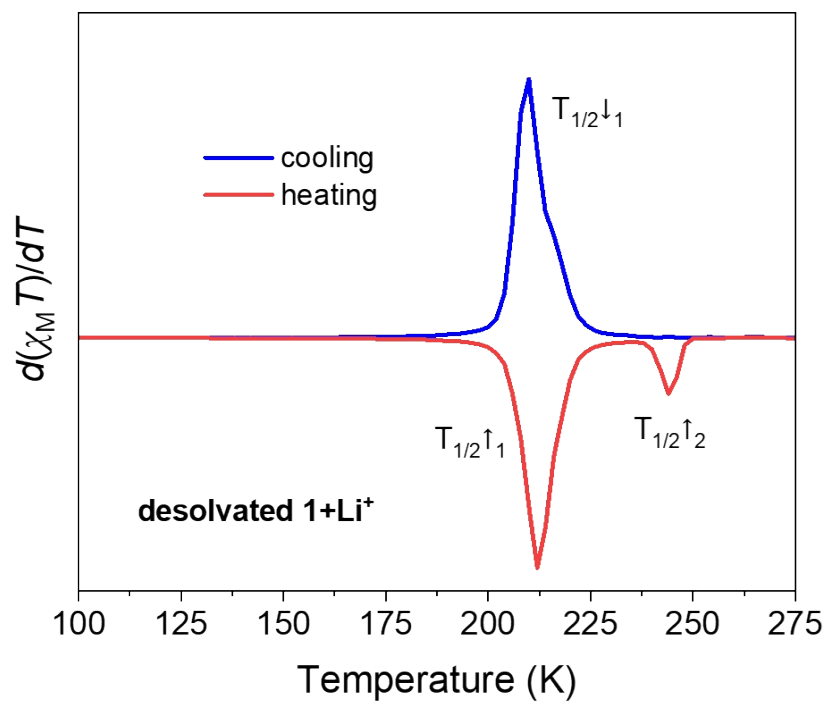


**Fig. S8** The first-order derivative of  $\chi_M T$  product for **1**+Li<sup>+</sup>.

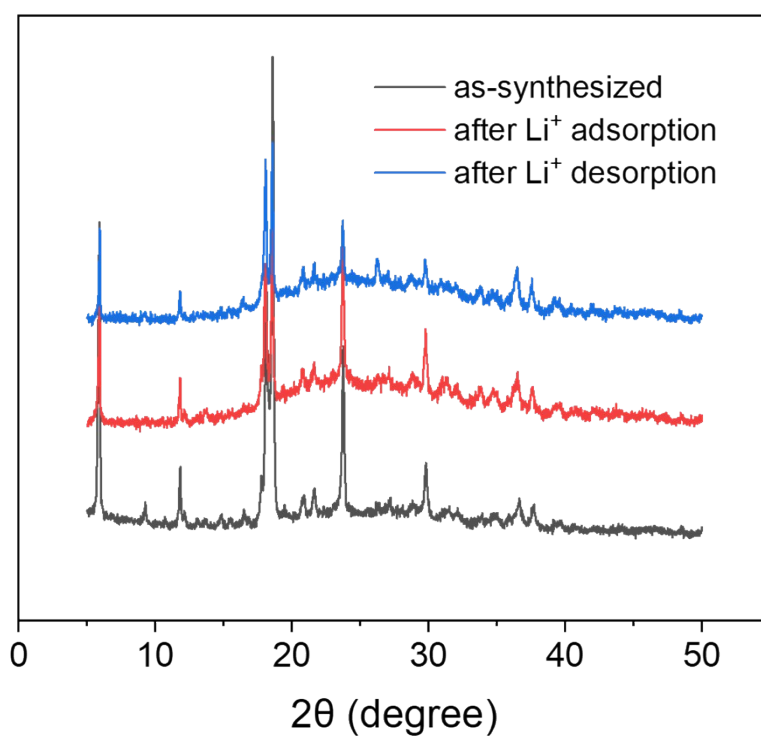


**Fig. S9** PXRD patterns of **1** upon Li<sup>+</sup> adsorption and desorption.

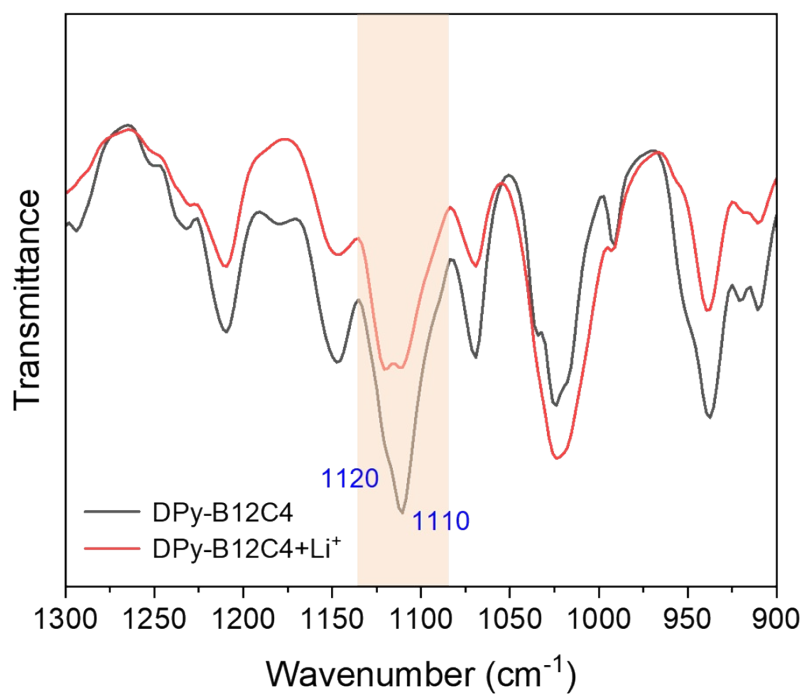
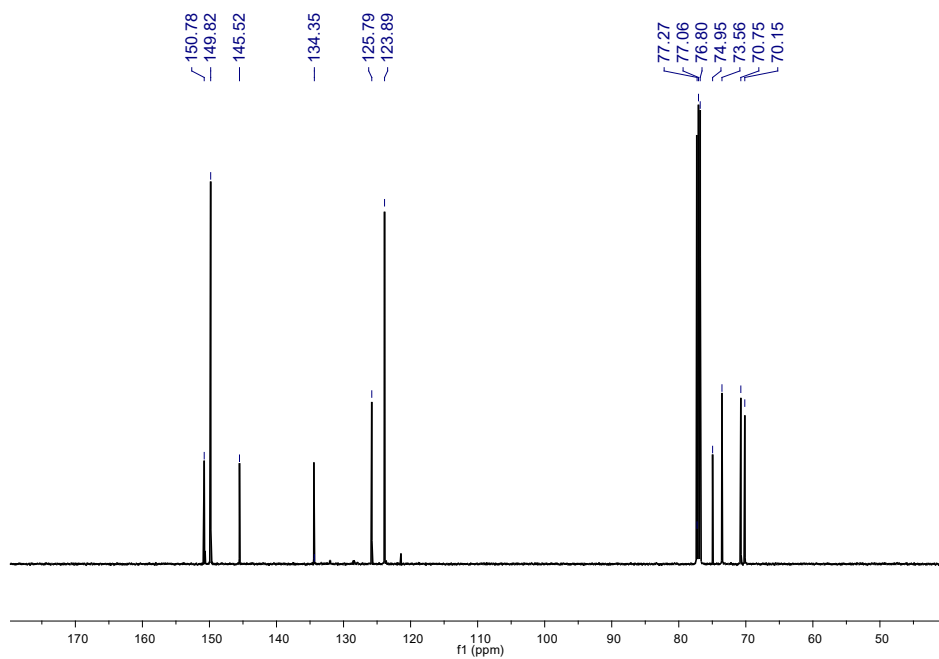
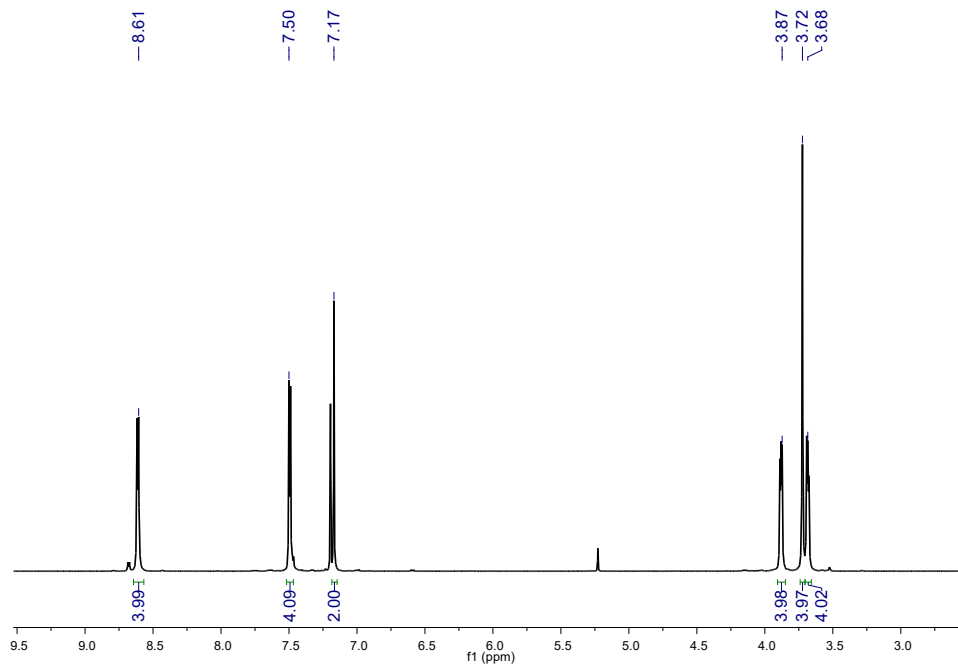


**Fig. S10.** FTIR spectra of free DPy-B12C4 ligand before and after Li<sup>+</sup> adsorption.

**Solution  $^1\text{H}$  and  $^{13}\text{C}$  NMR spectra of DPy-B12C4.**



## References

- (1) Frisch, M. J.; Trucks, G. W.; Schlegel, H. B.; Scuseria, G. E.; Robb, M. A.; Cheeseman, J. R.; Scalmani, G.; Barone, V.; Petersson, G. A.; Nakatsuji, H.; Li, X.; Caricato, M.; Marenich, A. V.; Bloino, J.; Janesko, B. G.; Gomperts, R.; Mennucci, B.; Hratchian, H. P.; Ortiz, J. V.; Izmaylov, A. F.; Sonnenberg, J. L.; Williams-Young, D.; Ding, F.; Lipparini, F.; Egidi, F.; Goings, J.; Peng, B.; Petrone, A.; Henderson, T.; Ranasinghe, D.; Zakrzewski, V. G.; Gao, J.; Rega, N.; Zheng, G.; Liang, W.; Hada, M.; Ehara, M.; Toyota, K.; Fukuda, R.; Hasegawa, J.; Ishida, M.; Nakajima, T.; Honda, Y.; Kitao, O.; Nakai, H.; Vreven, T.; Throssell, K.; Montgomery, J. A., Jr.; Peralta, J. E.; Ogliaro, F.; Bearpark, M. J.; Heyd, J. J.; Brothers, E. N.; Kudin, K. N.; Staroverov, V. N.; Keith, T. A.; Kobayashi, R.; Normand, J.; Raghavachari, K.; Rendell, A. P.; Burant, J. C.; Iyengar, S. S.; Tomasi, J.; Cossi, M.; Millam, J. M.; Klene, M.; Adamo, C.; Cammi, R.; Ochterski, J. W.; Martin, R. L.; Morokuma, K.; Farkas, O.; Foresman, J. B.; Fox, D. J. Gaussian, Inc., Wallingford CT, **2016**.
- (2) Shen, J.-C., Jiang, W.-L., Guo, W.-D., Qi, Q.-Y., Ma, D.-L., Lou, X.-B., Shen, M., Hu, B.-W., Yang, H.-B., Zhao, X. A rings-in-pores net: crown ether-based covalent organic frameworks for phase-transfer catalysis. *Chem. Commun.*, **2020**, *56*, 595-598.
- (3) Sheldrick, G. M. Crystal structure refinement with SHELXL. *Acta Crystallogr. Sect. C* **2015**, *71*, 3–8.
- (4) Dolomanov, O. V.; Bourhis, L. J.; Gildea, R. J.; Howard, J. A. K.; Puschmann, H. OLEX2: A complete structure solution, refinement and analysis program. *J. Appl. Crystallogr.* **2009**, *42*, 339–341.